# Endothelial nitric oxide synthase controls the expression of the angiogenesis inhibitor thrombospondin 2

Susan MacLauchlan[a,b], Jun Yu[a,c], Marcus Parrish[a], Tara A. Asoulin[a,b], Michael Schleicher[a,c], Marie M. Krady[a,b], Jianmin Zeng[a,b], Paul L. Huang[d], William C. Sessa[a,c], and Themis R. Kyriakides[a,b,1]

[a]Interdepartmental Program in Vascular Biology and Therapeutics, and Departments of [b]Pathology, and [c]Pharmacology, Yale University School of Medicine, New Haven, CT 06520; and [d]Cardiovascular Research Center and Cardiology Division, Massachusetts General Hospital, Boston, MA 02129

Edited* by Salvador Moncada, University College of London, London, United Kingdom, and approved September 1, 2011 (received for review March 18, 2011)

**Injury- and ischemia-induced angiogenesis is critical for tissue repair and requires nitric oxide (NO) derived from endothelial nitric oxide synthase (eNOS). We present evidence that NO induces angiogenesis by modulating the level of the angiogenesis inhibitor thrombospondin 2 (TSP2). TSP2 levels were higher than WT in eNOS KO tissues in hind-limb ischemia and cutaneous wounds. In vitro studies confirmed that NO represses TSP2 promoter activity. Moreover, double-eNOS/TSP2 KO mice were generated and found to rescue the phenotype of eNOS KO mice. Studies in mice with knock-in constitutively active or inactive eNOS on the Akt-1 KO background showed that eNOS activity correlates with TSP2 levels. Our observations of NO-mediated regulation of angiogenesis via the suppression of TSP2 expression provide a description of improved eNOS KO phenotype by means other than restoring NO signaling.**

wound healing | extracellular matrix | Akt | matrix metalloproteinases

Endothelial nitric oxide synthase (eNOS) and its bioactive product nitric oxide (NO) are well-established proangiogenic molecules. Endothelial-derived NO is crucial for maintenance of proper vasodilatory tone and regulation of an antiproliferative and antiapoptotic state for endothelial cells (ECs) and has essential roles in physiological angiogenesis (1–3). Pharmacological inhibition or genetic disruption of eNOS limited angiogenesis during tissue repair, resulting in delayed wound closure (2, 4). Addition of NO donors to wounds enhanced angiogenesis and accelerated healing (5–7). eNOS KO mice recovered poorly from hind-limb ischemia as a consequence of decreased angiogenesis (3, 8). These mice also displayed accelerated atherosclerosis, neointimal thickening postinjury, and hypertension (1, 9). Taken together, these observations highlight the ability of eNOS-derived NO to influence vascular function.

Thrombospondins (TSPs) are a small family of antiangiogenic matricellular proteins (10). TSPs enhance clearance of matrix metalloproteinase (MMP)-2 and MMP-9 (11–13) and interact with cell-surface receptors, including $\alpha_v\beta_3$, very low density lipoprotein receptor (VLDLR), CD36, and CD47, to inhibit angiogenesis (14). Further, ultrastructural studies demonstrated that TSP2 influences ECM assembly (15, 16). TSP2 KO mice displayed improved recovery of blood flow following ischemia (17), altered foreign body response (18, 19), and accelerated wound healing (16, 20, 21). In contrast, TSP1 KO mice displayed delayed healing because of insufficient stimulation of inflammation (13). Consistent with these observations, the expression of TSP1 and TSP2 in tissue repair was associated with the inflammatory and repair phases, respectively (13, 16). Recently, several studies linked components of the Akt-eNOS cascade with TSPs. Specifically, TSP1 has been described to blunt the ability of NO to activate soluble guanyl cyclase (sGC) (22, 23) through interactions with CD36 and CD47 during ischemia. TSP1 has also been described to diminish eNOS activity by blocking phosphorylation at S1176 (24). Studies in retina angiogenesis connected oxidative stress and regulation of TSP2. In this model, the production of TSP2 was directly correlated with the levels of reactive oxygen species (ROS) (25, 26). However, the mechanism regulating TSP2 expression was not described. Finally, in a tumor model, Akt-1 KO mice displayed increased vessel density associated with decreased TSP1 and TSP2 in a manner directly correlated with Akt-1 activation (27). This paradoxical observation of increased angiogenesis in Akt-1 KO mice was attributed to the specific conditions of the tumor model. In addition, wound healing in Akt-1 KO mice was compromised because of decreased VEGF availability, decreased vascularity, and altered collagen assembly and maturation in dermal wound beds (28). However, TSP1 and TSP2 expression in this model was not evaluated; thus, it was not clear if the compromised phenotype was associated with alterations in their expression.

Because of the opposite phenotypes of eNOS KO and TSP2 KO mice in tissue repair and the developing evidence that there exists a NO-TSP axis, we initiated studies to investigate associations between eNOS and TSP2. Analysis of ischemic and wound tissues from eNOS KO mice revealed significantly increased TSP2 levels. In vitro studies allowed us to determine that NO-mediated depression of TSP2 occurred by means of a transcriptional effect. The functional role of increased TSP2 in eNOS KO animals was explored by generating TSP2/eNOS double-null mice. These mice displayed increased recovery of blood flow following ischemia and accelerated wound healing. Finally, we investigated the role of the Akt-eNOS axis in modulating TSP2 expression and observed increased TSP2 deposition in the wounds of Akt-1 KO and eNOS S11766A/Akt-1 KO knock-in mice. In contrast, TSP2 deposition was decreased in the wounds of eNOS S1176D/Akt-1 KO mice, suggesting that eNOS activity inversely correlates with TSP2 expression. Thus, these data demonstrate that the proangiogenic actions of NO occur, in part, via modulation of the levels of the antiangiogenic molecule TSP2 and the loss of TSP2 rescues a deficiency in eNOS-derived NO.

## Results

**eNOS-KO Tissues and Cells Have Increased TSP2 Levels.** TSP2 expression is low in uninjured tissues and is induced following hind-limb ischemia, with maximum expression at 1 wk (17). At 2 wk

Author contributions: S.M., J.Y., M.S., M.M.K., W.C.S., and T.R.K. designed research; S.M., J.Y., M.P., T.A.A., M.S., M.M.K., J.Z., and T.R.K. performed research; P.L.H. contributed new reagents/analytic tools; S.M., J.Y., T.A.A., W.C.S., and T.R.K. analyzed data; and S.M., W.C.S., and T.R.K. wrote the paper.

The authors declare no conflict of interest.

*This Direct Submission article had a prearranged editor.

[1]To whom correspondence should be addressed. E-mail: themis.kyriakides@yale.edu.

See Author Summary on page 18585.

This article contains supporting information online at www.pnas.org/lookup/suppl/doi:10.1073/pnas.1104357108/-/DCSupplemental.

postischemia, TSP2 levels in WT animals are low in the ischemic leg (left calf) and almost undetectable in the uninjured leg (right calf) (Fig. 1*E*). In contrast, Western blot analysis of eNOS KO tissues revealed increased TSP2 protein in both the ischemic and nonischemic legs at 2 wk following ischemia (Fig. 1*E*). Immunohistochemical analysis of muscle sections revealed increased TSP2 in eNOS KO muscles before injury (day 0, Fig. 1*B*) and at 2 wk following ischemia (Fig. 1*D*) compared with WT (Fig. 1 *A* and *C*). Furthermore, the distribution of TSP2 was altered, because blood vessels, which are typically void of TSP2 (Fig. 1*C*), displayed TSP2 immunoreactivity (Fig. 1*D*). eNOS KO tissue 2 wk following ischemia displayed TSP2 expression associated with muscle fibers, fibroblasts, and capillaries.

Similar to ischemic tissues, TSP2 deposition was increased in eNOS KO dermal wounds. Specifically, at day 10 after cutaneous wounding, which is the peak of TSP2 expression in WT mice (16), eNOS KO wounds displayed significantly increased TSP2 deposition by immunohistochemistry (Fig. 1 *F* and *G*). Western blots of day 10 wound extracts and densitometry also showed that TSP2 levels were increased 1.3-fold in eNOS KO wounds

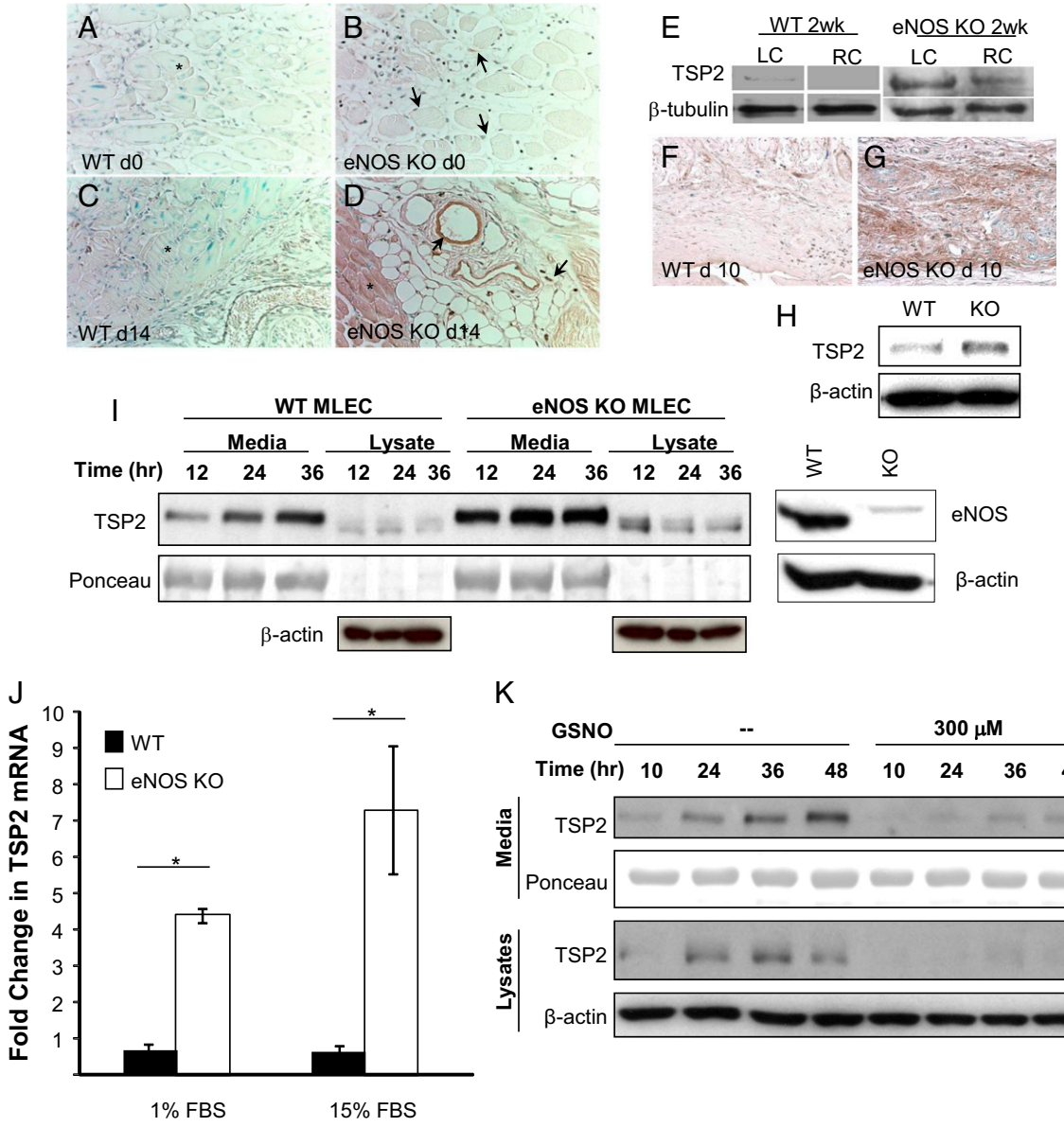


**Fig. 1.** Increased TSP2 levels in eNOS KO mice. Representative images of gastrocnemius muscles from day 0 (*A* and *B*) and day 14 (*C* and *D*) ischemic WT (*A* and *C*) and eNOS KO (*B* and *D*) mice immunostained for TSP2 and visualized by the peroxidase reaction (brown color) are shown. Nuclei were counterstained with methylene green. Arrows in *B* indicate immunoreactive cells. Arrows in *D* indicate the presence of TSP2 immunostain on small and large vessels. In the latter, the levels of TSP2 were elevated (compare *C* and *D*). Muscle fibers are denoted by an asterisk. (*E*) Western blot analysis of muscle extracts from WT and eNOS KO mice at 2 wk postsurgery shows increased TSP2 expression in both ischemic [left calf (LC)] and nonischemic [right calf (RC)] muscles. Representative images of day 10 dermal wounds from WT (*F*) and eNOS KO (*G*) mice immunostained for TSP2 are shown. The latter display an increased level of TSP2 deposition. (Magnification: 400×.) (*H*) Western blot analysis of day 10 extracts from WT and eNOS KO wounds reveals increased TSP2 in the latter. (*I*) Western blot analysis of TSP2 in conditioned media and cell lysates of WT and eNOS MLECs for the indicated times in hours. (*Right*) Western blot analysis for eNOS in the MLECs to verify KO. (*J*) eNOS KO MLECs have increased TSP2 mRNA as determined by RT-PCR. Data are expressed as average ± SEM. *$P \leq 0.05$ (DKO vs. eNOS KO). (*K*) Western blot analysis of TSP2 in conditioned media and cell lysates of eNOS KO MLECs treated with the NO donor GSNO (100 and 250 μm) for the indicated times. Ponceau-S and β-actin are shown as loading controls in media and lysate samples, respectively.

(Fig. 1*H*). Consistent with a previous report (2), we observed compromised wound closure in eNOS KO animals. Because we have previously shown that the levels of MMPs in wounds are inversely correlated with TSP2 (29, 30), we analyzed day 10 wounds extracts by zymography and found reduced levels of MMP-9 and normal levels of MMP-2 in eNOS KO wounds (Fig. S1*A*). Immunohistochemical analysis of wounds confirmed the reduced levels of MMP-9 (Fig. S1*C*).

To verify the in vivo relationship between eNOS and TSP2 levels, mouse lung endothelial cells (MLECs) were isolated from WT and eNOS KO animals and analyzed for TSP2 production by Western blotting. Consistent with our in vivo findings, eNOS KO MLECs produced more TSP2 than WT MLECs (Fig. 1*I*). Increased levels were observed in both the amount of TSP2 secreted into MLEC media as well as intracellular TSP2 in cell lysates (Fig. 1*I*). TSP2 mRNA levels in eNOS KO MLECs were also increased relative to WT (Fig. 1*J*). Furthermore, the upregulation of TSP2 was reversed by addition of an exogenous NO donor, S-nitrosoglutatione (GSNO) (Fig. 1*K*). Specifically, levels of TSP2 in eNOS KO MLEC-conditioned media, as well as the amount of TSP2 in cell lysates, were decreased over time with the addition of GSNO (300 μM). These data suggest that autocrine NO might serve as means by which ECs endogenously suppress TSP2 expression.

**NO Regulates TSP2 in a Paracrine Fashion by Decreasing TSP2 Expression.** The major cell types that synthesize TSP2 in vivo are fibroblasts, pericytes, and smooth muscle cells (20). Our in vivo assays demonstrated that lack of eNOS-derived NO resulted in increased TSP2 levels. To assess whether NO altered TSP2 levels in vitro in a paracrine fashion, fibroblasts, which are the major TSP2 producers in vivo, were treated with the NO donors GSNO and diethylenetriamine NONOate [DETANONOate (DETANO)]. Less TSP2 was secreted into the media by National Institutes of Health 3T3 cells (NIH3T3s) treated with GSNO or DETANO during a period of 24 h (Fig. 2 *A* and *B*). During the same time course, NO donor-treated NIH3T3s also decreased intracellular TSP2. The earliest detectable decrease in TSP2 accumulation into cell media was at 3 h in the presence of GSNO and 6 h in DETANO-treated cells, and the reduction was maintained throughout the entire 24 h. At 1 mM DETANO, which has a half-life between 20 and 24 h and releases two molar equivalents of NO per mole of DETANO compound (31), the effective dose of NO has been measured to be between 0.9 and 1.5 μM NO (32). Effective DETANO and GSNO concentrations were determined by performing a dose–response experiment (Fig. S2 *A* and *B*). The effect of NO donor on TSP2 production was confirmed in other cell types, including human primary fibroblasts (Fig. S2*C*).

To exclude the possibility that the effect of NO donor was attributable to reactive nitrogen species (RNS), we treated cells with DETANO and 2-(4-carboxyphenyl)-4,5-dihydro-4,4,5,5–tetramethyl-1H-imidazolyl-1-oxy-3- oxide (CPTIO) in combination (Fig. S3). CPTIO binds to NO and generates $NO_2$. Treatment of NIH3T3s with CPTIO and DETANO did not enhance the efficacy of DETANO alone, indicating that the decrease in TSP2 is attributable to NO and not to RNS. The antioxidant ascorbic acid did not have an effect on TSP2 expression and did not reverse the effect of DETANO, suggesting that oxidative stress does not influence TSP2 production (Fig. S4*A*). The canonical target for NO is activation of sGC. ODQ, a pharmacological inhibitor of sGC, did not prevent NO-mediated reduction of TSP2 (Fig. S4*B*), indicating that the NO effect on TSP2 production is cGMP-independent.

To determine DETANO effects on TSP2 protein stability, DETANO was added to cells transfected with TSP2 plasmid. HEK293 cells, which produce undetectable levels of TSP2, were transfected with empty vector (pcDNA3) or TSP2. DETANO (0–1 mM) did not decrease TSP2 expression in HEK293 lysates

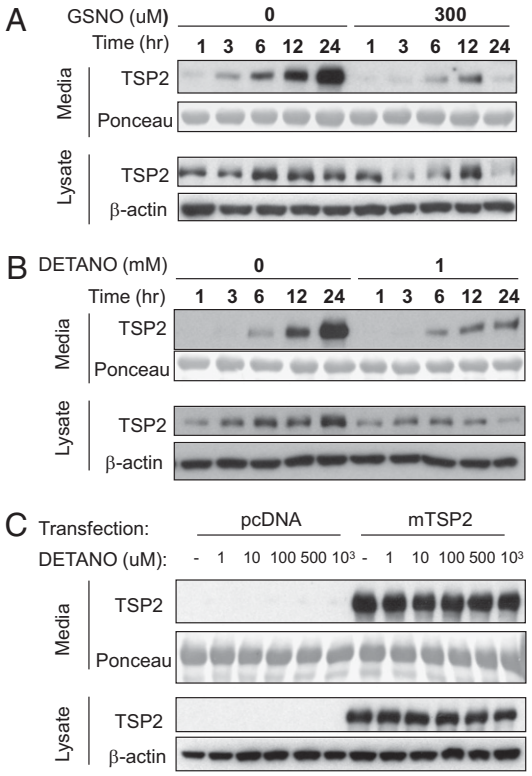


**Fig. 2.** Exogenous NO reduces TSP production in a paracrine manner. (*A*) Western blot analysis of TSP2 in conditioned media and cell lysates of NIH3T3s cultured in the presence or absence of 300 μm of GSNO for the indicated times. (*B*) Western blot analysis of TSP2 in conditioned media and cell lysates of NIH3T3s cultured in the presence or absence of 1 mM DETANO for the indicated times. (*C*) Western blot analysis of TSP2 in conditioned media and cell lysates in HEK293 epithelial cells transfected with pcDNA (vector control) or mTSP2 cDNA. Cells were treated with increasing concentrations of DETANO. Ponceau-S and β-actin are shown as loading controls in media and lysate samples, respectively.

or media after 24 h of treatment (Fig. S5). Even at the highest dose of DETANO (1 mM), intracellular and secreted TSP2 levels were unchanged throughout a time course of 24 h (Fig. 2*C*). Because the plasmid-derived TSP2 was insensitive to DETANO, we conclude that NO decreases TSP2 mRNA levels via a transcriptional effect.

TSP2 mRNA was quantified following DETANO treatment and was significantly decreased, in comparison to untreated cells, at 12 h and further depressed at 24 h (Fig. 3*A*). To ensure that the effect on TSP2 mRNA was not attributable to global changes in transcription, several other mRNA targets were tested after 24 h of DETANO treatment. Fibronectin, collagen IIIα1, and MMP-9 mRNA levels were unchanged with DETANO treatment, but collagen Iα1 mRNA was decreased by 80% (Fig. 3*B*). Our findings show that DETANO specifically decreases certain mRNA, including TSP2 and collagen Iα1. DETANO did not alter the rate of decay of TSP2 mRNA following actinomycin-D treatment, indicating that it did not affect mRNA stability (Fig. 3*C*). Luciferase assays verified that the observed decrease in TSP2 mRNA level was attributable to decreased transcriptional activity. Following DETANO treatment of NIH3T3s for 24 h, TSP2 promoter activity was decreased by half relative to untreated cells (Fig. 3*D*).

**TSP2 Deficiency Rescues the eNOS-KO Phenotype in Ischemia and Dermal Wound Healing.** To investigate the impact of increased TSP2 in eNOS KO mice, double-eNOS/TSP2 KO (DKO) mice

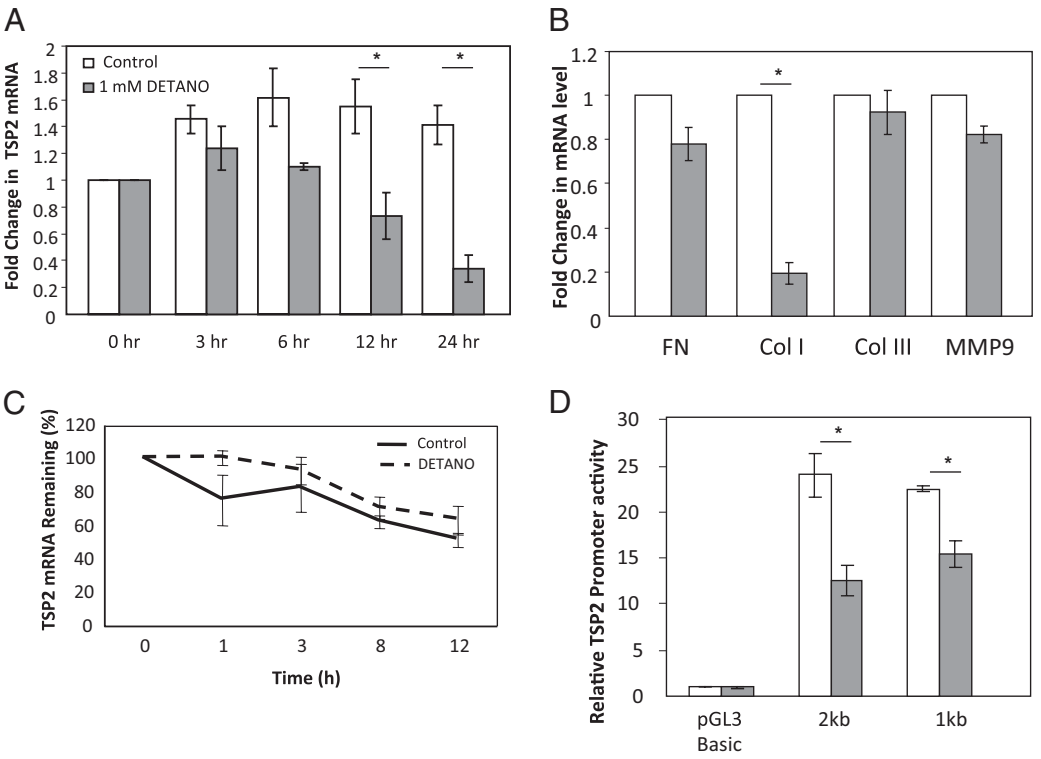


**Fig. 3.** NO reduces TSP2 mRNA transcription. (*A*) Qualitative RT-PCR analysis of TSP2 mRNA levels in NIH3T3s cultured in the presence (gray bars) or absence (white bars) of 1 mM DETANO for the indicated times. (*B*) Qualitative RT-PCR analysis of various mRNA levels in NIH3T3s cultured in the presence or absence of 1 mM DETANO for 24 h. (*C*) NIH3T3s were treated with actinomycin-D, and the decay of TSP2 mRNA in the absence and presence of 1 mM DETANO was assessed by qualitative RT-PCR and expressed as a percentage of the original for the time indicated. (*D*) NIH3T3s were cotransfected with SV40 renilla and test luciferase plasmid (the promoterless pGL3 basic or the TSP2 promoter) and either untreated or treated with DETANO (1 mM) for 24 h. Data are expressed as normalized to pGL3 luciferase expression and normalized to SV40 renilla. In all figures, data are expressed ± SEM. *$P \leq 0.05$ DETANO treatment relative to untreated NIH3T3s.

were generated by breeding the two single-null lines. Mice were confirmed by genotyping as well as mRNA and protein analysis (Fig. S6 *A* and *B*). Tissue repair in these mice was evaluated in hind-limb ischemia and full-thickness dermal wounds. eNOS KO mice recover poorly from hind-limb ischemia, typically resulting in severe necrosis and loss of limb (3), and do not restore blood flow to the ischemic limb (Fig. 4*A*), whereas blood flow in WT mice returns to preinjury levels by 4 wk. In comparison to single-eNOS KO mice, DKO mice displayed improved restoration of blood flow in the ischemic limb (Fig. 4*A*). A possible explanation for the lack of complete recovery in these mice involves the profound ischemia and necrosis they experience in the first 2–4 d as well as TSP2-independent effects of eNOS. As we showed previously, TSP2 is not expressed in WT ischemic muscle during this time frame (17). Thus, its deletion in the DKO mice cannot overcome the severe early phenotype. Enumeration of blood vessels in ischemic muscles at 2 and 4 wk revealed increased angiogenesis in the DKO mice (Fig. 4*B*). Previously, we demonstrated the presence of an enhanced arterial network in TSP2 KO mice. Consistent with this observation, anti-smooth muscle actin immunohistochemistry revealed the enhanced presence of collaterals in the uninjured muscles of DKO mice in comparison to eNOS KO mice (5.1 ± 1.4 vs. 2.9 ± 1.1; $P \leq 0.05$).

In an excisional dermal wound healing model, deletion of TSP2 reversed and improved the eNOS KO phenotype. Specifically, DKO wounds displayed efficient closure associated with reduction in the wound area and the appearance of specialized structures, such as sweat glands and hair follicles, in the area of the wound (Fig. 4 *C–H*). Similar to the ischemia model, early healing in DKO mice appeared to be compromised, as evident in the larger wound areas and delayed wound reepithelialization at day 5 (Fig. S6*C*). However, DKO wounds displayed dramatic improvement associated with increased angiogenesis and ECM remodeling between days 7 and 10, a time when TSP2 expression is maximal in WT wounds (Fig. S6 *D* and *E*). Consistent with previous observations in TSP2 KO mice, Masson's trichrome stain revealed that wounds in DKO mice had irregular deposition of collagen fibers with loose basket-weave morphology (13) (Fig. 4 *I–K*).

**Akt-eNOS Axis Regulates TSP2 Expression.** Expression of eNOS in ECs is constitutive and its activity can be regulated by multiple kinases. We asked whether Akt-1, the major eNOS kinase in ECs (33, 34), could also influence TSP2 expression by determining the level of TSP2 in dermal wounds in Akt-1 KO mice. Immunohistochemical analysis revealed significantly increased TSP2 deposition in Akt-1 KO mice at day 10 posthealing compared with WT mice (Fig. 5*A*). To confirm the involvement of reduced eNOS activation in this process, we used Akt-1 KO mice with knock-in mutations of eNOS mimicking gain of function or loss of function (S1176D and S1176A, respectively) (34). Analysis of excisional wounds revealed healing rates dependent on eNOS activity (Fig. 5). Moreover, TSP2 distribution was inversely proportional to predicted NO levels (Fig. 5 *B* and *C*). Specifically, Akt-1 KO and eNOS S1176A/Akt-1 KO wounds healed slower and had increased TSP2 deposition (Fig. 5). In contrast, TSP2 expression was reduced in eNOS S1176D/Akt-1 KO wounds and healing was accelerated. Western blot analysis of day 10 wounds and densitometry indicated a 1.6-fold decrease in

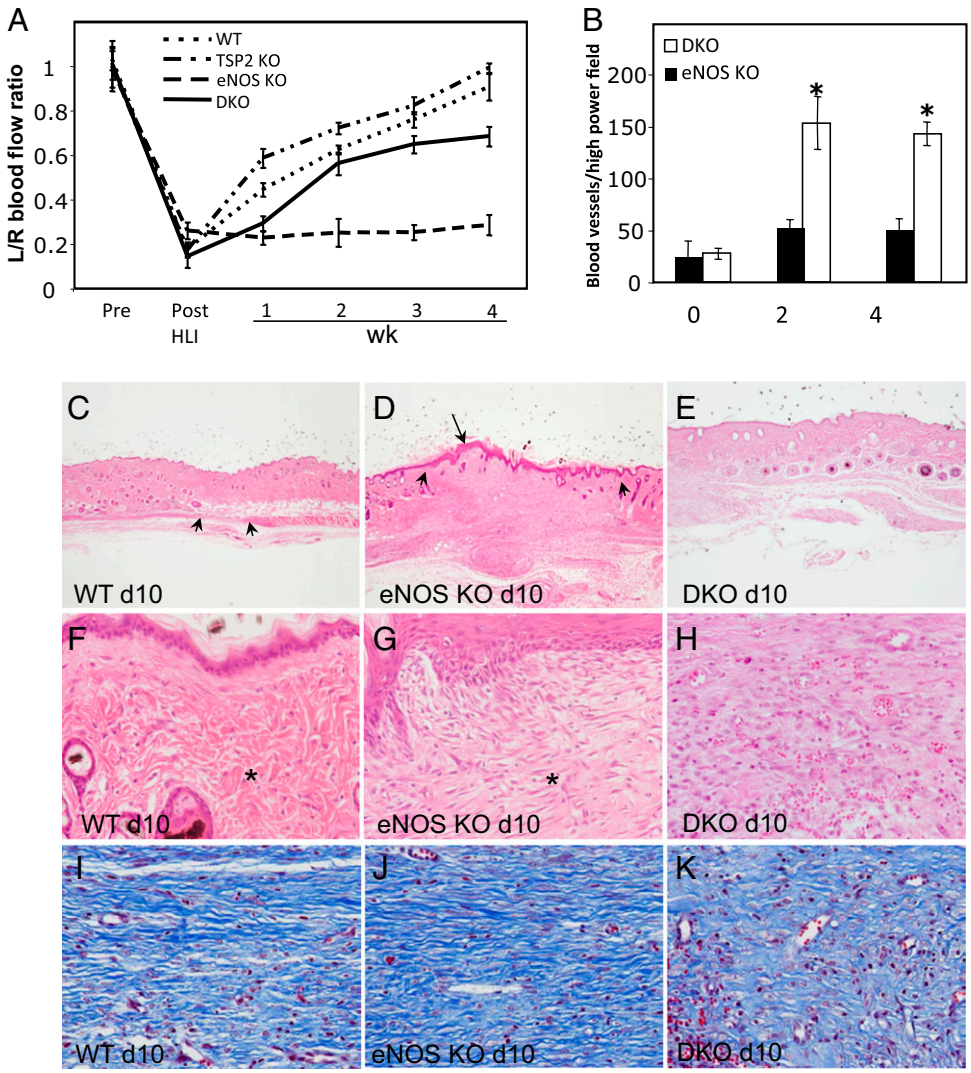


**Fig. 4.** DKO mice display improved ischemia-initiated blood flow recovery and improved wound healing. (*A*) Blood flow in the gastrocnemius muscle of 3-mo-old mice was measured at 1–4 wk using a deep-penetrating laser Doppler probe and expressed as the ratio of the left limb (ischemic) relative to the right limb (nonischemic). The ratio before surgery was 1. (*B*) Quantification of PECAM-1–positive vascular structures indicated increased angiogenesis in DKO muscles at 2 and 4 wk. Data are expressed as blood vessels per high-power field and denote ± SEM. *$P \leq 0.05$ eNOS KO compared with DKO. Representative low- and high-power images of H&E-stained sections from day 10 wounds in WT (*C* and *F*), eNOS KO (*D* and *G*), and DKO (*E* and *H*) mice are shown. Delayed healing is associated with the presence of thickened epithelium and immature ECM in eNOS KO wounds. Arrowheads in *C* and *D* indicate wound margins. The arrow in *D* indicates thickened epithelium. Asterisks in *F* and *G* indicate collagenous matrix in the wound bed. High-power images of Masson's trichrome-stained representative sections of day 10 wounds from WT (*I*), eNOS KO (*J*), and DKO (*K*) mice reveal irregular collagen deposition (blue color) in the latter ($n = 6$). (Magnification: *C–E*, 40×; *F–H*, 100×; *I–K*, 400×.)

TSP2 levels in the eNOS S1176D/Akt-1 KO mice relative to the eNOS S1179A/Akt-1 KO mice (Fig. 5*E*). Taken together, these observations suggest that the Akt/eNOS axis regulates the expression of TSP2. Moreover, zymographic analysis of day 10 wound extracts and immunohistochemical analysis revealed increased MMP-9 in eNOS S1176D/Akt-1 KO mice relative to eNOS S1176A/Akt-1 KO mice (Fig. S1 *D–F*). Consistent with our findings in eNOS KO mice, we did not detect a significant difference in MMP-2 levels.

## Discussion

NO has been extensively studied regarding its proangiogenic roles in endothelial homeostasis, migration, proliferation, and tube formation. Many NO-sensitive factors have been identified via in vitro analyses. In this study, we present evidence that regulation of TSP2 transcription is an effector of NO. Specifically, we show that TSP2 is overexpressed in eNOS KO ischemic and wound tissues and that this expression is restored in a manner consistent with the levels of eNOS activity. The functional significance of increased TSP2 in eNOS KO mice was evaluated by generation of DKO animals, which displayed an improved healing phenotype. These observations suggest that TSP2 is a bona fide NO target and propose a previously undescribed proangiogenic mechanism for NO through transcriptional repression of a major antiangiogenic molecule. In an eNOS KO background, TSP2 deletion reverses the severe eNOS KO wound-healing phenotype and partially restores the ischemic phenotype. Previously, we showed that TSP2 deficiency does not influence collagen levels but is associated with aberrant morphology and assembly of collagen fibrils and fibers, respectively. Consistent with these observations, we observed the deposition of aberrantly organized collagen fibers in DKO wounds. These data provide genetic evidence for the physiological importance of the eNOS-TSP2 axis. TSP2 deficiency has also been associated

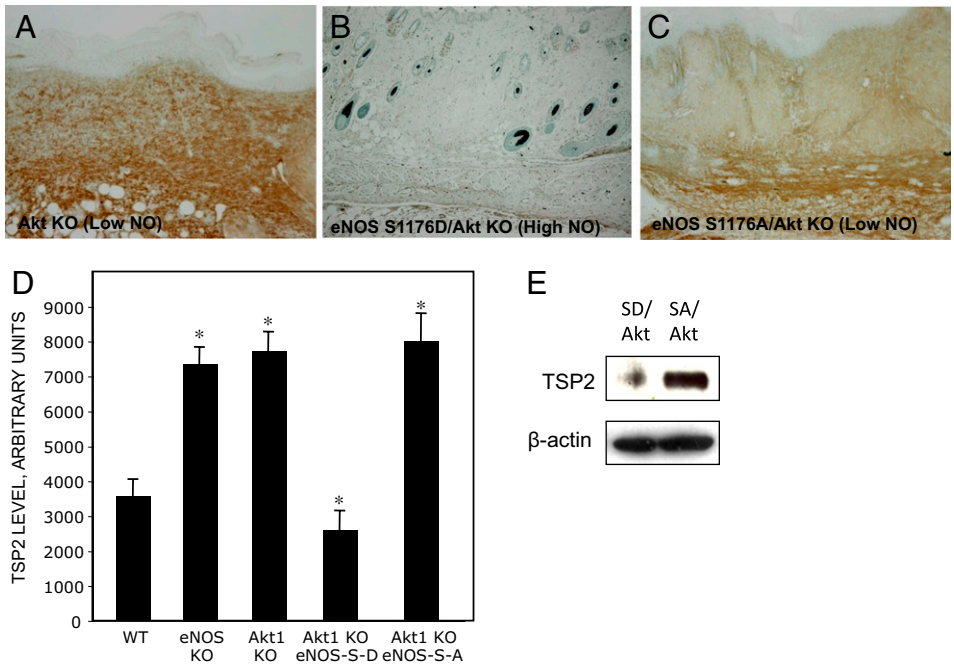


**Fig. 5.** Regulation of TSP2 expression by the Akt-eNOS axis. Representative sections stained for TSP2 by immunohistochemistry in day 10 wounds in Akt-1 KO (*A*), eNOS S1176D/Akt-1 KO (*B*), and eNOS S1176A/Akt-1 KO (*C*) mice and counterstained with methylene green are shown. (Magnification: 100×.) (*D*) Quantitation of TSP2 immunohistochemical staining analyzed in Metamorph ± SEM. *$P \leq 0.05$ relative to WT. (*E*) Western blot analysis of day 10 wound extracts also reveals decreased TSP2 in eNOS S1176D/Akt-1 KO wounds relative to eNOS S1176A/Akt-1 KO wounds.

with increased levels of MMP-2 and MMP-9 in various models of tissue repair (35). In the present study, we observed that the increased TSP2 in eNOS KO wounds was associated with reduced MMP-9 levels and that this finding was reversed in eNOS S1176D/Akt-1 KO mice. It is unclear why we observed changes only in MMP-9, but others have made similar observations in TSP2 KO heart infarcts following angiotensin treatment (36). Taken together, because of the ability of TSP2 to modulate cell-matrix interactions, our data support a role for NO in regulating ECM assembly. More importantly, our findings provide previously undescribed insight into the regulation of TSP2 transcription.

Molecular mechanisms regulating NO-mediated effects are not completely understood. Here, we present data showing that NO controls angiogenesis indirectly by repressing the expression of TSP2. There are conflicting data suggesting that NO can influence the expression of other angiogenesis inhibitors, such as angiostatin. For example, in a canine coronary ischemia model, angiostatin levels were increased in nitro-L-arginine methyl ester hydrochloride (L-NAME)–treated animals (37). This increase was associated with enhanced MMP-2 and MMP-9 activity. However, another study demonstrated that rats treated with L-NAME for 6 wk exhibited no change in MMP or angiostatin levels (38). Differences in these studies could stem from the role of NO in the two models; whereas the canine model is ischemia-driven, the rat study had no injurious stimuli. Secretion of another antiangiogenic protein, endostatin, was induced in response to hydrogen peroxide, chemically induced hypoxia, or NO treatment and was decreased with NOS inhibition (39). However, these observations were limited to an in vitro model and the intracellular mechanism for NO was not investigated.

Recently, several groups described TSP1 as an antagonist for NO signaling. TSP1 attenuates activation of sGC mediated by either eNOS or exogenous NO sources (22, 23). Unlike this well-documented effect of TSP1 on NO signaling, little is known about the role of NO in the regulation of TSP1 or TSP2 levels. Exogenous NO-treated kidney mesangial cells decreased TSP1 mRNA (40). Treatment of human umbilical chord endothelial cells with DETANO demonstrated suppression of secreted TSP1, and this effect was independent of sGC activation and ERK phosphorylation (41). Because TSP1 and TSP2 are encoded by distinct genes with unique promoters (42), we hypothesize that the NO-mediated suppression is distinct. Indeed, our results excluded sGC activation as a means of down-regulating TSP2 (Fig. S4). However, because sGC expression is frequently lost in vitro, we cannot exclude that this might be a factor controlling TSP2 expression in vivo. In this study, we examined several cell types, including MLECs and fibroblasts, none of which produced sufficient TSP1 to achieve detection by Western blotting. In contrast, implantation of melanoma cells into Akt-1 KO mice resulted in tumors with decreased TSP1 and TSP2 levels, and ECs transfected with either dominant-negative Akt or myristoylated Akt were correlated with decreased and increased TSP1, respectively (27). However, this study did not investigate the role of eNOS in influencing TSP levels vs. the multiple other Akt-1 targets in the cell. In the same study, the reduced levels of TSPs in Akt-1 KO mice were shown to be associated with increased tumor angiogenesis (27). Moreover, Akt-1 had a positive effect on TSP2 transcription, and a preparation of lung ECs from Akt KO mice, which contained 30% fibroblasts, had decreased TSP1 and TSP2 levels. However, the authors mentioned that there was not a substantial eNOS component in their tumor model and that the strain of Akt KO mice used in their study had only a modest decrease in NO production (27). In contrast, in our study, both the wound healing and ischemia models are dependent on NO and are compromised in eNOS KO and Akt-1 KO mice. Thus, differences in mouse strains and the variable dependence of angiogenic models on NO might explain the conflicting observations regarding TSP2 levels. In fact, in a separate study, the same group showed compromised angiogenesis in wound healing (28). However, despite the previous association of Akt-1 deficiency with reduced TSPs, which was the major

finding in the tumor study, the authors did not provide data regarding TSP1 or TSP2 levels in Akt-1 KO wounds (28). Based on our own observations, we conclude that NO plays a critical role in the negative regulation of TSP2 during tissue repair.

The ability of NO to regulate TSP2 expression has not been reported previously. However, a link between oxidative stress and TSP2 has been established in a model in which deletion of CYP1B1 resulted in increased ROS and TSP2 in retinal-derived ECs, which was reversed with an antioxidant (25, 43). Moreover, TSP2 redox sensitivity is confirmed by the observation that Rac1-induced ROS increased TSP2 in human aortic endothelial cells (HAECs) (26). Here, we show that TSP2 expression is not altered by antioxidant treatment, which might be attributable to cell specificity. More importantly, unlike the studies outlined above, we demonstrate that NO directly effects TSP2 transcription. Because our in vitro assays required sustained slow-releasing NO donor, such as GSNO or DETANO, it is possible that NO levels exceeded those required in vivo. In fact, NO concentration in tissue is typically in the nanomolar range. It is difficult to experimentally deliver low-dose, long-term NO. Addition of DETANO and CPTIO in combination suggests that NO, rather than RNS, controls TSP2 levels. However, because CPTIO alone was insufficient to restore DETANO-mediated decreased TSP2 production, it is possible that other NO species in high concentrations also depress TSP2 (Fig. S2).

TSP2 can influence cell function via the modulation of cell-matrix interactions and matrix assembly. Although not an integral component of collagen fibrils, TSP2 has been shown to regulate collagen fibrillogenesis, leading to autocrine and paracrine effects on cell function (15, 17). Our studies suggest that NO may influence ECM assembly and ultrastructure, which has not been described before. Previous studies in cultured mesangial cells showed that either NO stimulated through iNOS induction or exogenous GSNO altered levels of ECM molecules, including decreased collagen (type 1α1 and type 1α2), fibronectin, and TSP1, and increased laminin (40, 44). The participation of NO in ECM synthesis was also demonstrated in an anti–Thy1-induced kidney damage model, where treatment with a phosphodiesterase 5 (PDE5) inhibitor, a cGMP catabolizing enzyme, displayed decreased collagen IV, fibronectin, and TSP1 (45). Although this study did not evaluate the effect of NO directly on ECM, it demonstrates that ECM production can be affected by the NO-generated second-messenger cGMP. NO-mediated reduction in collagen levels has been confirmed in cell types relevant to wound healing and ischemia, including fibroblasts and smooth muscle cells (46–48). NO has also been described to alter expression and/or activity of several MMPs (49–51), specifically MMP-2, MMP-9, and MMP-13. Consistent with these studies, our data demonstrate that NO decreased the mRNA levels of both collagen I, a major ECM constituent, as well as TSP2, which would be expected to have significant effects on ECM assembly. This suggestion is supported by the observation of reduced MMP-9 levels in eNOS KO wounds.

Activation of Akt/eNOS signaling leads to generation of NO and proangiogenic activity. Based on our findings, we propose an additional effect for this signaling axis involving the transcriptional repression of TSP2. The importance of TSP2 in the context of low NO levels is underscored by the fact that the DKO mice have substantial restoration in healing. Thus, we conclude that increased TSP2 has negative consequences on healing and is an important regulator of the eNOS KO phenotype. We also believe that our findings of improved repair in the DKO mice cannot be solely ascribed to the loss of the antiangiogenic effect of TSP2 because we have already shown that the lack of TSP2 does not improve the vascularization and healing of wounds in TSP1/TSP2 KO DKO mice (13). Moreover, increased expression of TSP2 in Akt-1 KO wounds provides additional support for the importance of the Akt/eNOS axis in the regulation of TSP2 expression. In addition to eNOS, Akt-1 activates a diverse range of targets and influences cell growth, survival, and migration (52). However, modulation of eNOS activity in Akt-1 KO wounds was sufficient to change TSP2 and MMP-9 levels and promote healing. Taken together, our observations show that modulation of TSP2 expression is a major function of NO and a significant outcome of Akt-eNOS signaling.

## Methods

**Animals.** The generation of TSP2 KO mice (53), eNOS KO mice (Jackson Laboratory), and eNOS S1176A/Akt-1 KO and eNOS S1176D/Akt-1 KO mice (34) has been described previously. DKO animals were generated by breeding of homozygotes. Matched WT littermates were generated using the same breeding scheme. DKO genotyping was confirmed by PCR analysis of tail DNA and Western blot analysis of tissue as described elsewhere (2, 15). All experiments were approved by the Institutional Animal Care and Use Committee at Yale University.

**Reagents.** GSNO was produced by nitrosylation of GSH (Sigma) and DETANO was purchased from Alexis Biochemicals. L-ascorbate acid was obtained from the Wako Chemical Company. ODQ and CPTIO were purchased from Cayman Chemicals.

**Ischemia.** Hind-limb ischemia was performed as previously described (3, 33). Briefly, mice were anesthetized (100 mg/kg of ketamine and 10 mg/kg of xylazine) and ischemia was induced in the left leg by ligation of both the proximal portion of the femoral artery and the distal portion of the saphenous artery. Branches between the two sites were ligated or cauterized, and arteriectomy was performed. Skin incision without femoral artery ligation was also performed as a sham operation. Blood flow was measured by means of a Doppler perfusion unit (Periflux system; Perimed). Deep muscle flow was measured using a deep measurement probe placed directly onto the gastrocnemius muscle. Perfusion was determined in both the ischemic and nonischemic limbs before surgery; directly after surgery; and at 1, 2, 3, and 4 wk postsurgery. The reported blood flow value represents the ratio of ischemic to nonischemic hind-limb perfusion. A total of six mice per time point per genotype were analyzed.

**Wounds.** Full-thickness excisional wounds were made in the dorsal region of mice anesthetized with Avertin, as described previously (16). Each mouse received two 6-mm wounds with the aid of a biopsy punch (Acuderm), producing a total of 10 wounds per time point. All wounds were excised with a 3-mm rim of unwounded tissue. The first wound was administered on day 0 and the second on day 7. A total of 6 wounds per time point per genotype were made.

**Tissue Processing and Analysis.** Excised wounds were fixed in 10% (vol/vol) zinc-buffered formalin (Z-fix; Anatech) and embedded in paraffin. Five-micrometer-thick sections were generated and stained with H&E, Masson's trichrome, anti-TSP2, and anti–MMP-9, and immunohistochemistry was performed as described previously (13, 15, 19, 21). The specificity of each antibody was verified previously using tissues from TSP2 KO and MMP-9 KO mice (13, 54, 54). Immune reactions, based on peroxidase activity, were visualized with the Vector ABC Elite kit (Vector Laboratories). A Nikon Eclipse 800 microscope equipped with fluorescence optics was used for all examinations. Metamorph software (Molecular Devices) was used to determine the relative intensity of the peroxidase activity.

Protein extracts from day 10 wounds were prepared in extraction buffer as described previously (13). The protein content of each sample was determined by a BCA assay, according to the supplier's instructions (Bio-Rad). A total of six samples per genotype were analyzed, and the experiment was performed twice. Antibodies (TSP2, β-actin, and β-tubulin) were used for Western blot analysis as described previously (17). Blot densitometry was analyzed using Image J (National Institutes of Health), calculated as the densitometry of TSP2 signal normalized to the densitometry of the associated β-actin band densitometry, and expressed as normalized to the indicated genotypes. Gelatin zymography of wound extracts was performed as described previously, and zymograms were reversed to visualize MMPs as dark bands (21).

**Cell Culture.** NIH3T3s and HEK293 cells (American Type Culture Collection) were maintained in DMEM (Gibco) supplemented with 10% (vol/vol) FBS, penicillin, streptomycin, and L-glutamine. MLECs were isolated and immortalized as previously described (33, 55). MLECs were cultured in EBM-2 media

(Lonza) with 15% (vol/vol) HyClone-characterized FBS (Thermo Scientific), EGM-2MV SingleQuot growth factors (Cambrex), penicillin, streptomycin, and 2× L-glutamine.

Primary human dermal fibroblasts (a gift from Marty Kluger, Yale University, New Haven, CT) were maintained in DMEM supplemented with 10% (vol/vol) FBS and penicillin, streptomycin, and L-glutamine. Fibroblasts were cultured to 80% confluence in six-well plates and switched to starve media (DMEM with 0.5% FBS) in the presence and absence of GSNO (300 μM). At indicated times after GSNO addition, media and lysates were collected and analyzed by Western blotting for TSP2 and β-actin.

**Cell Transfection.** Cells were transfected using Lipofectamine (Invitrogen) and Optimem (Gibco) as indicated by manufacturers. HEK293 cells plated in six-well plates were transfected with 1 μg per well of empty pcDNA3 vector (Invitrogen) or mTSP2 pcDNA3 (plasmid 12411; Addgene.org). The following day, cells were washed with PBS and transferred to antibiotic-free starvation media and DETANO at the indicated concentration.

**Media and Intracellular Lysate Generation and Western Blot Analysis.** Experiments were performed with cells at 80% confluence. Cells were switched to starve media (DMEM + 0.5% FBS or EGM-2 + 1% serum for fibroblasts or ECs, respectively) in the presence of a given concentration of NO donors [GSNO was generated by nitrosylation of glutathione by sodium nitrite (DETANO; Alexis Biochemicals)]. GSNO was generated and used with exclusion of light. Over the given ranges, cells did not demonstrate visual indications of apoptosis. Media and cell lysates were collected at times following NO donor addition. Cells were lysed in radioimmunoprecipitation assay buffer plus protease inhibitors (Complete Mini EDTA-free inhibitor mixture; Roche). Western blot analysis was performed using TSP2 (BD Bioscience) and β-actin (Sigma) as described previously.

**RNA Isolation and Qualitative RT-PCR.** RNA samples were collected using the RNeasy Mini Kit (Qiagen). RT was performed on 1 μg of RNA (Superscript II; Invitrogen) using OligodT and Random Hexamer (Invitrogen) primers. SYBRgreen (BioRad) semiquantitative PCR was performed using a BioRad iCycler5. Primers were designed using the National Center for Biotechnology Information's primer design tool or were replicated from literature references (available on request). Samples were run in duplicate and averaged. Experimental results reflect the average of triplicate experiments. For the mRNA stability assay, NIH3T3s were pretreated with actinomycin-D (1 μg/mL for 30 min; Sigma–Aldrich) in starve media before addition of DETANO. RNA was isolated after DETANO addition over a period of 12 h. RT and qualitative PCR were performed as above. The experiment was performed three times. Data were normalized to GAPDH and expressed as percent message remaining relative to actinomycin-D–treated cells ($t = 0$). Although GAPDH expression is described to decrease in certain systems, the addition of DETANO changed GAPDH expression less than one-fold within any given experiment.

**Luciferase Assay.** For luciferase transfections, NIH3T3s plated in 12-well plates were cotransfected with a luciferase construct (pGL3 basic, 200 ng per well; Promega) or mTSP2 promoter construct and SV40 renilla (50 ng per well). The transfection mixture was added to cells in antibiotic-free starve media in the absence and presence of 1 mM DETANO. After transfection for 24 h, the Dual Luciferase Reporter Assay (Promega) was performed according to the manufacturer's suggestion, and samples were assayed on a Lumat luminometer (Berthold Technologies). This assay was performed four times in duplicate.

**Statistical Analysis.** Data are presented as mean ± SEM. Student's *t* tests were performed on the data comparing untreated and NO-treated samples, and significance was determined at $P \leq 0.05$. Statistical differences in the ischemia data were determined using two-way ANOVA, followed by Bonferroni's post hoc test. A $P$ value $\leq 0.05$ was considered to be statistically significant.

**ACKNOWLEDGMENTS.** We thank Dr. Kurt Hankenson (University of Pennsylvania) for the 2-kb TSP2 promoter construct. This work was funded by National Institutes of Health Grant GM-072194-01 (to T.R.K). S.M. is funded by American Heart Association Predoctoral Grant 09PRE2080166.

1. Rudic RD, et al. (1998) Direct evidence for the importance of endothelium-derived nitric oxide in vascular remodeling. *J Clin Invest* 101:731–736.
2. Lee PC, et al. (1999) Impaired wound healing and angiogenesis in eNOS-deficient mice. *Am J Physiol* 277:H1600–H1608.
3. Yu J, et al. (2005) Endothelial nitric oxide synthase is critical for ischemic remodeling, mural cell recruitment, and blood flow reserve. *Proc Natl Acad Sci USA* 102:10999–11004.
4. Schaffer MR, Tantry U, Gross SS, Wasserburg HL, Barbul A (1996) Nitric oxide regulates wound healing. *J Surg Res* 63:237–240.
5. Zhu H, Wei X, Bian K, Murad F (2008) Effects of nitric oxide on skin burn wound healing. *J Burn Care Res* 29:804–814.
6. Schäffer MR, et al. (1997) Nitric oxide, an autocrine regulator of wound fibroblast synthetic function. *J Immunol* 158:2375–2381.
7. Witte MB, Thornton FJ, Efron DT, Barbul A (2000) Enhancement of fibroblast collagen synthesis by nitric oxide. *Nitric Oxide* 4:572–582.
8. Murohara T, et al. (1998) Nitric oxide synthase modulates angiogenesis in response to tissue ischemia. *J Clin Invest* 101:2567–2578.
9. Kuhlencordt PJ, et al. (2001) Accelerated atherosclerosis, aortic aneurysm formation, and ischemic heart disease in apolipoprotein E/endothelial nitric oxide synthase double-knockout mice. *Circulation* 104:448–454.
10. Bornstein P (2009) Thrombospondins function as regulators of angiogenesis. *J Cell Commun Signal* 3:189–200.
11. Yang Z, Kyriakides TR, Bornstein P (2000) Matricellular proteins as modulators of cell-matrix interactions: Adhesive defect in thrombospondin 2-null fibroblasts is a consequence of increased levels of matrix metalloproteinase-2. *Mol Biol Cell* 11: 3353–3364.
12. Hahn-Dantona E, Ruiz JF, Bornstein P, Strickland DK (2001) The low density lipoprotein receptor-related protein modulates levels of matrix metalloproteinase 9 (MMP-9) by mediating its cellular catabolism. *J Biol Chem* 276:15498–15503.
13. Agah A, Kyriakides TR, Lawler J, Bornstein P (2002) The lack of thrombospondin-1 (TSP1) dictates the course of wound healing in double-TSP1/TSP2-null mice. *Am J Pathol* 161:831–839.
14. Kyriakides TR, Maclauchlan S (2009) The role of thrombospondins in wound healing, ischemia, and the foreign body reaction. *J Cell Commun Signal* 3:215–225.
15. Kyriakides TR, et al. (1998) Mice that lack thrombospondin 2 display connective tissue abnormalities that are associated with disordered collagen fibrillogenesis, an increased vascular density, and a bleeding diathesis. *J Cell Biol* 140:419–430.
16. Kyriakides TR, Tam JW, Bornstein P (1999) Accelerated wound healing in mice with a disruption of the thrombospondin 2 gene. *J Invest Dermatol* 113:782–787.
17. Krady MM, et al. (2008) Thrombospondin-2 modulates extracellular matrix remodeling during physiological angiogenesis. *Am J Pathol* 173:879–891.
18. Kyriakides TR, Leach KJ, Hoffman AS, Ratner BD, Bornstein P (1999) Mice that lack the angiogenesis inhibitor, thrombospondin 2, mount an altered foreign body reaction characterized by increased vascularity. *Proc Natl Acad Sci USA* 96:4449–4454.
19. Kyriakides TR, Zhu YH, Yang Z, Huynh G, Bornstein P (2001) Altered extracellular matrix remodeling and angiogenesis in sponge granulomas of thrombospondin 2-null mice. *Am J Pathol* 159:1255–1262.
20. Agah A, Kyriakides TR, Letrondo N, Björkblom B, Bornstein P (2004) Thrombospondin 2 levels are increased in aged mice: Consequences for cutaneous wound healing and angiogenesis. *Matrix Biol* 22:539–547.
21. Maclauchlan S, et al. (2009) Enhanced angiogenesis and reduced contraction in thrombospondin-2-null wounds is associated with increased levels of matrix metalloproteinases-2 and -9, and soluble VEGF. *J Histochem Cytochem* 57:301–313.
22. Isenberg JS, et al. (2006) CD47 is necessary for inhibition of nitric oxide-stimulated vascular cell responses by thrombospondin-1. *J Biol Chem* 281:26069–26080.
23. Isenberg JS, Martin-Manso G, Maxhimer JB, Roberts DD (2009) Regulation of nitric oxide signalling by thrombospondin 1: Implications for anti-angiogenic therapies. *Nat Rev Cancer* 9:182–194.
24. Bauer EM, et al. (2010) Thrombospondin-1 supports blood pressure by limiting eNOS activation and endothelial-dependent vasorelaxation. *Cardiovasc Res* 88:471–481.
25. Tang Y, et al. (2009) CYP1B1 expression promotes the proangiogenic phenotype of endothelium through decreased intracellular oxidative stress and thrombospondin-2 expression. *Blood* 113:744–754.
26. Lopes N, et al. (2003) Thrombospondin 2 regulates cell proliferation induced by Rac1 redox-dependent signaling. *Mol Cell Biol* 23:5401–5408.
27. Chen J, et al. (2005) Akt1 regulates pathological angiogenesis, vascular maturation and permeability in vivo. *Nat Med* 11:1188–1196.
28. Somanath PR, Chen J, Byzova TV (2008) Akt1 is necessary for the vascular maturation and angiogenesis during cutaneous wound healing. *Angiogenesis* 11:277–288.
29. Tian W, Sawyer A, Kocaoglu FB, Kyriakides TR (2011) Astrocyte-derived thrombospondin-2 is critical for the repair of the blood-brain barrier. *Am J Pathol* 179:860–868.
30. Krady M, et al. (2008) Thrombospondin-2 modulates extracellular matrix remodeling during physiological angiogenesis. *Am J Pathol* 173:879–891.
31. Keefer LK, Nims RW, Davies KM, Wink DA (1996) "NONOates" (1-substituted diazen-1-ium-1,2-diolates) as nitric oxide donors: Convenient nitric oxide dosage forms. *Methods Enzymol* 268:281–293.
32. Borutaite V, Brown GC (2003) Nitric oxide induces apoptosis via hydrogen peroxide, but necrosis via energy and thiol depletion. *Free Radic Biol Med* 35:1457–1468.
33. Ackah E, et al. (2005) Akt1/protein kinase Balpha is critical for ischemic and VEGF-mediated angiogenesis. *J Clin Invest* 115:2119–2127.
34. Schleicher M, et al. (2009) The Akt1-eNOS axis illustrates the specificity of kinase-substrate relationships in vivo. *Sci Signal* 2:ra41.
35. Kyriakides TR, Maclauchlan S (2009) The role of thrombospondins in wound healing, ischemia, and the foreign body reaction. *J Cell Commun Signal* 3:215–225.

36. Schroen B, et al. (2004) Thrombospondin-2 is essential for myocardial matrix integrity: Increased expression identifies failure-prone cardiac hypertrophy. *Circ Res* 95:515–522.
37. Matsunaga T, et al. (2002) Angiostatin inhibits coronary angiogenesis during impaired production of nitric oxide. *Circulation* 105:2185–2191.
38. Frisbee JC, Samora JB, Basile DP (2007) Angiostatin does not contribute to skeletal muscle microvascular rarefaction with low nitric oxide bioavailability. *Microcirculation* 14:145–153.
39. Deininger MH, et al. (2003) Endothelial endostatin release is induced by general cell stress and modulated by the nitric oxide/cGMP pathway. *FASEB J* 17:1267–1276.
40. Wani J, Carl M, Henger A, Nelson PJ, Rupprecht H (2007) Nitric oxide modulates expression of extracellular matrix genes linked to fibrosis in kidney mesangial cells. *Biol Chem* 388:497–506.
41. Ridnour LA, et al. (2005) Nitric oxide regulates angiogenesis through a functional switch involving thrombospondin-1. *Proc Natl Acad Sci USA* 102:13147–13152.
42. Shingu T, Bornstein P (1993) Characterization of the mouse thrombospondin 2 gene. *Genomics* 16:78–84.
43. Tang Y, et al. (2009) CYP1B1 and endothelial nitric oxide synthase combine to sustain proangiogenic functions of endothelial cells under hyperoxic stress. *Am J Physiol Cell Physiol* 298(3):C665–C678.
44. Trachtman H, Futterweit S, Singhal P (1995) Nitric oxide modulates the synthesis of extracellular matrix proteins in cultured rat mesangial cells. *Biochem Biophys Res Commun* 207:120–125.
45. Hohenstein B, Daniel C, Wittmann S, Hugo C (2008) PDE-5 inhibition impedes TSP-1 expression, TGF-beta activation and matrix accumulation in experimental glomerulonephritis. *Nephrol Dial Transplant* 23:3427–3436.
46. Dooley A, et al. (2007) Effect of nitric oxide and peroxynitrite on type I collagen synthesis in normal and scleroderma dermal fibroblasts. *Free Radic Biol Med* 43: 253–264.
47. Myers PR, Tanner MA (1998) Vascular endothelial cell regulation of extracellular matrix collagen: Role of nitric oxide. *Arterioscler Thromb Vasc Biol* 18:717–722.
48. Kolpakov V, Gordon D, Kulik TJ (1995) Nitric oxide-generating compounds inhibit total protein and collagen synthesis in cultured vascular smooth muscle cells. *Circ Res* 76:305–309.
49. Ridnour LA, et al. (2007) Nitric oxide regulates matrix metalloproteinase-9 activity by guanylyl-cyclase-dependent and -independent pathways. *Proc Natl Acad Sci USA* 104: 16898–16903.
50. Zaragoza C, Balbín M, López-Otín C, Lamas S (2002) Nitric oxide regulates matrix metalloprotease-13 expression and activity in endothelium. *Kidney Int* 61:804–808.
51. Jurasz P, et al. (2001) Matrix metalloproteinase 2 in tumor cell-induced platelet aggregation: Regulation by nitric oxide. *Cancer Res* 61:376–382.
52. Shiojima I, Walsh K (2002) Role of Akt signaling in vascular homeostasis and angiogenesis. *Circ Res* 90:1243–1250.
53. Kyriakides TR, Zhu YH, Yang Z, Bornstein P (1998) The distribution of the matricellular protein thrombospondin 2 in tissues of embryonic and adult mice. *J Histochem Cytochem* 46:1007–1015.
54. Tian W, Kyriakides TR (2009) Matrix metalloproteinase-9 deficiency leads to prolonged foreign body response in the brain associated with increased IL-1beta levels and leakage of the blood-brain barrier. *Matrix Biol* 28:148–159.
55. Kuhlencordt PJ, et al. (2004) Role of endothelial nitric oxide synthase in endothelial activation: Insights from eNOS knockout endothelial cells. *Am J Physiol Cell Physiol* 286:C1195–C1202.